Three-sphere low-Reynolds-number swimmer near a wall

Rojman Zargar,[1] Ali Najafi,[2,*] and MirFaez Miri[1,†]
[1]*Institute for Advanced Studies in Basic Sciences (IASBS), P.O. Box 45195-1159, Zanjan 45195, Iran*
[2]*Department of Physics, Zanjan University, Zanjan 313, Iran*
(Received 11 February 2009; published 19 August 2009)

We study the influence of a wall on the dynamics of a low-Reynolds-number three-sphere swimmer. A far swimmer whose arm makes an angle θ with the horizon experiences the wall presence as an angle-dependent quadrupole force proportional to $(a/L)^2(L/z)^2\cos\theta$, where a, L, and z are the radius of spheres, the arm length, and the swimmer distance to the wall, respectively. The wall-induced translational velocity of swimmer is perpendicular to the arms. A far swimmer prefers to orient its arms parallel to the plate. This state is stable. Remarkably, the parallel state is unstable when the swimmer is close to the wall. In this regime, the velocity of swimmer decreases as $(z/L)^2$. Numerical solution of the equations of motion for arbitrary initial z/L and θ reveals four different phases of locomotion.

DOI: 10.1103/PhysRevE.80.026308 PACS number(s): 47.15.G−, 87.19.ru, 45.40.Ln

I. INTRODUCTION

Design and fabrication of artificial molecular machines are the subject of growing experimental and theoretical investigations [1,2]. Such machines with their ability to transport, mix, and sort materials are involved in biophysical and microfluidic applications [3]. Smart nanocarriers can deliver and trigger the release of active agents in the cellular environments [4]. In microfluidic devices with their crucial applications in drug discovery [5], nanopumps and nanomotors are the basic elements [6].

A simple design of a nanomachine favors its realization with the currently available technologies. In nature, biological microorganisms, such as bacteria, have fascinating mechanisms to swim at very low Reynolds number [7]. Thus, biologically inspired propellers are the basic proposal for locomotion in fluids.

In his pioneering work, Taylor [8] modeled the microorganism propulsion by a train of two-dimensional sinusoidal waves traveling across an inextensible sheet. Purcell in his seminal work proposed the simplest swimmer with two internal degrees of freedom [9]. The propulsion velocity of Purcell's three-link swimmer is calculated recently [10]. Stroke patterns of this swimmer are optimized to achieve maximum efficiency [11]. There are also many works devoted to microswimmers based on nonreciprocal deformations [12,13], phoretic effects, and chemical reactions [14] and linked magnetic beads controlled by an external magnetic field [15].

A simple swimmer, which is a different geometrical version of Purcell's system, is introduced in Ref. [16]. The swimmer consists of a central sphere that is connected to two other spheres with straight rods [17]. The system moves by varying the length of arms in a periodic but time irreversible manner. The three-sphere swimmer has attracted much attention since it captures almost the whole characteristics of a low-Reynolds-number propeller, and it consists of spherical objects whose hydrodynamic interactions are extensively studied. N-sphere swimmers that can change both the length of their arms and the angle between them [18], mutual hydrodynamic interactions between two three-sphere swimmer [19], the role of noise and coherence in the stroke cycle [20], a conformation kinetic model to drive the deformation cycle [21], and a swimmer with one of the spheres having a larger radius [22] are thoroughly studied. Recently, Leoni *et al.* experimentally realized the three-sphere low-Reynolds-number swimmer [23].

Swimming in a geometrically confined environment is a subject of growing interest [24–29]. A plethora of fascinating phenomena emerges due to hydrodynamic interactions of the swimmer with solid surfaces. Even for a single sphere, the diffusion parallel to the wall is always bigger than the perpendicular diffusion [30], which has been verified experimentally [31]. Experiments also show that microorganisms, e.g., E. coli [32], bull spermatozoa [33], and human spermatozoa [34] swimming in confined geometries are attracted by surfaces. Apparently, understanding the migration of infectious bacteria along medically implanted surfaces such as catheters and prostheses [35], the movement of bacteria through the pores of saturated soil [36], the migration of bacteria through small-diameter capillary tubes [37] are important. In the realm of microfluidics, walls are expected to have a profound effect on the motion of fluids and propellers.

Inspired by the above-mentioned systems and in view of designing a drug carrier moving in small-diameter capillaries, we study the mutual interaction between the three-sphere low-Reynolds-number swimmer and a rigid wall. The advantage of focusing on this model propeller is that hydrodynamic interactions between a sphere and a wall and between two spheres are known. Our study paves the way for understanding hydrodynamic interactions between a propeller and walls of a channel of rectangular cross section. Our results can be examined by a simple extension of the recent experiment of Leoni *et al.*

The rest of the paper is organized as follows. In Sec. II we introduce the three-sphere swimmer near a wall. Section III is devoted to the formulation of the problem. The results of two different cases, where swimmer is far from and close to the wall, are presented in Sec. IV. Concluding remarks are given in Sec. V.

*najafi@znu.ac.ir
†miri@iasbs.ac.ir

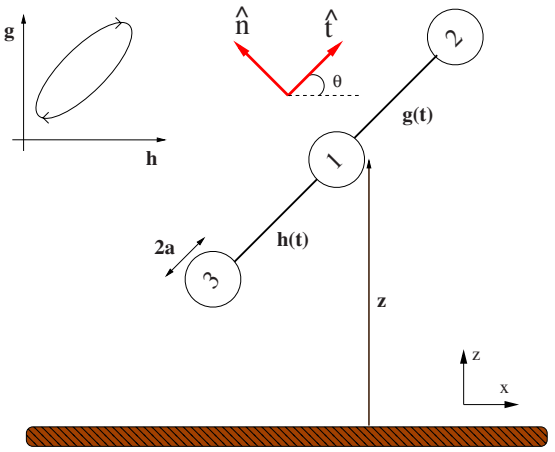

FIG. 1. (Color online) Schematic view of a three-sphere swimmer near a wall. The unit vector $\hat{t}$ shows the arm direction. Top left: an admissible nonreciprocal motion in the (h,g) space.

II. MODEL: A THREE-SPHERE SWIMMER NEAR A WALL

To quantify the relative importance of the inertial and frictional effects, Reynolds has introduced a dimensionless number. The Reynolds number $\mathcal{R}$ in terms of typical length scale l, typical velocity v, fluid density ρ, and fluid viscosity η, which are characteristics of the flow, is $\mathcal{R}=\rho v l/\eta$. For an artificial propeller swimming in water, $l\approx 1-10$ μm, $v\approx 1-10$ μm/s, $\rho\approx 1000$ kg/m^3, and $\eta\approx 10^{-3}$ Pa s; thus, $\mathcal{R}\approx 10^{-6}-10^{-4}$ is quite low.

Propulsive motion in the highly viscous conditions, where the viscous effects dominate over the inertia effects, is not a trivial task [9]. Under these conditions, any swimming mechanism should involve a *nonreciprocal* cyclic motion. The nonreciprocal motion breaks the time-reversal symmetry and is of prime importance in swimming.

Figure 1 shows a schematic view of a simple three-sphere swimmer moving in a fluid medium bounded by a wall. The swimmer consists of three spheres linked by two arms of negligible diameter. The length of arms denoted by $h(t)$ and $g(t)$ varies in a nonreciprocal manner to have a net displacement. We use the internal deformation space (h,g) to draw a simple picture of the possible swimming mechanisms. Any closed path in this space involves a sequence of body deformations, which propels the system. In particular, a simple elliptic path in this space is a periodic variation in the arm lengths, with a constant phase difference between the deformations of two arms.

$\mathbf{x}_i$ and $\dot{\mathbf{x}}_i$ are the position vector and velocity of the ith sphere $(i=1,2,3)$, respectively, that characterize the space configuration and dynamical behavior of the three-sphere system. Because of the symmetry considerations and with no loss of generality, we analyze the motion of swimmer in a two-dimensional space (x,z) (see Fig. 1). In the following, we first set up low-Reynolds-number hydrodynamic description of the system and then solve the equations of motion.

III. HYDRODYNAMIC INTERACTIONS BETWEEN THE SWIMMER AND WALL

Stokes equation describes the fluid motion at zero Reynolds number. Denoting the fluid velocity field by $\mathbf{u}(\mathbf{r})$, the pressure by $p(\mathbf{r})$, and the force density acting on the fluid by $\mathbf{f}(\mathbf{r})$, the Stokes equation reads as $-\eta\nabla^2\mathbf{u}(\mathbf{r})+\nabla p(\mathbf{r})=\mathbf{f}(\mathbf{r})$ [30]. The conservation of mass for the incompressible fluid can be expressed as $\nabla\cdot\mathbf{u}(\mathbf{r})=0$. The velocity field is also subject to a no-slip boundary condition on rigid surfaces.

One of the elementary solutions to the Stokes equation is the velocity field of a point force $\mathbf{f}(\mathbf{r})=\mathbf{b}\delta(\mathbf{r}-\mathbf{r}_0)$ embedded in the infinite space and this solution is called Stokeslet or Oseen-Burgers tensor. The velocity field of the Stokeslet can be written as $\mathbf{u}(\mathbf{r})=G(\mathbf{r}-\mathbf{r}_0)\cdot\mathbf{b}$, where the *free space* Green's function of the Stokes equation reads as

$$G^F_{\alpha\beta}(\mathbf{r}-\mathbf{r}_0)=\frac{1}{8\pi\eta}\left(\frac{\delta_{\alpha\beta}}{x}+\frac{x_\alpha x_\beta}{x^3}\right), \tag{1}$$

here $\mathbf{x}=\mathbf{r}-\mathbf{r}_0$ and $\alpha,\beta=1,2,3$.

In 1971, Blake obtained the velocity field due to a point force in the vicinity of a stationary plane boundary [38]. Since the no-slip condition should be satisfied on the plane, the influence of the boundary on the flow is deep. Assuming that the wall is located at $z=0$ and the point force resides in $\mathbf{r}_0$, the following form for the Green's function can be written as

$$\begin{aligned}G^B_{\alpha\beta}(\mathbf{r}-\mathbf{r}_0)=\frac{1}{8\pi\eta}\Bigg[&\left(\frac{\delta_{\alpha\beta}}{x}+\frac{x_\alpha x_\beta}{x^3}\right)-\left(\frac{\delta_{\alpha\beta}}{R}+\frac{R_\alpha R_\beta}{R^3}\right)\\&+2z_0^2(1-2\delta_{\beta z})\left(\frac{\delta_{\alpha\beta}}{R^3}-\frac{3R_\alpha R_\beta}{R^5}\right)-2z_0(1-2\delta_{\beta z})\\&\times\left(\frac{R_z}{R^3}\delta_{\alpha\beta}-\frac{R_\beta}{R^3}\delta_{\alpha z}+\frac{R_\alpha}{R^3}\delta_{\beta z}-\frac{3R_\alpha R_\beta R_z}{R^5}\right)\Bigg].\end{aligned} \tag{2}$$

Here $\mathbf{x}=\mathbf{r}-\mathbf{r}_0$, $z_0=\hat{z}\cdot\mathbf{r}_0$, $\mathbf{R}=\mathbf{r}-\mathbf{r}_0^i$, and $\mathbf{r}_0^i$ represents the image point of $\mathbf{r}_0$ with respect to the wall.

Let us assume that a collection of N spherical objects are moving inside the fluid. We denote by $\mathbf{f}_i$ the hydrodynamic force acting on the ith sphere moving with velocity $\mathbf{v}_i$. The force and velocities of spheres obey the equations

$$\mathbf{v}_i=\sum_{j=1}^{N}M_{ij}\cdot\mathbf{f}_j, \tag{3}$$

where the mobility tensors M_{ij} express the response of the ith sphere to the force acting on the jth sphere. We can use Faxén's theorem for spherical objects with radius a to express the mobility tensor in terms of the Green's function of Stokes equation [30,39],

$$M^{\alpha\beta}_{ij}=\left(1+\frac{a^2}{6}\nabla^2_{\mathbf{r}_i}\right)\left(1+\frac{a^2}{6}\nabla^2_{\mathbf{r}_j}\right)G^{\alpha\beta}(\mathbf{r}_i,\mathbf{r}_j). \tag{4}$$

If we assume that the radius a is smaller than the distance between spheres then $M^{\alpha\beta}_{ij}=G^{\alpha\beta}(\mathbf{r}_i,\mathbf{r}_j)$ up to the second order in a. It follows immediately that the Green's function $G^B_{\alpha\beta}(\mathbf{r}_i,\mathbf{r}_j)$ introduced by Blake is the first approximation for the mobility tensor of spheres moving in a fluid bounded by a wall.

Another point to mention is the self-mobility of a sphere moving near a wall. Assuming that the distance z between sphere and wall is greater than the sphere radius a, the components of self-mobility tensor are [30,39]

$$M_{ii}^{xx} = \mu_0\left(1 - \frac{9}{16}\frac{a}{z}\right),$$

$$M_{ii}^{zz} = \mu_0\left(1 - \frac{9}{8}\frac{a}{z}\right), \tag{5}$$

where $\mu_0 = 1/(6\pi\eta a)$.

IV. INFLUENCE OF WALL ON THE KINEMATICS OF THREE-SPHERE SWIMMER

In this section, we describe equations governing the dynamics of a three-sphere swimmer adjacent to a plane. The hydrodynamic force and torque acting on the ith sphere are denoted by $\mathbf{f}_i$ and $\boldsymbol{\tau}_i$, respectively. Equation (3) relates the velocity $\dot{\mathbf{x}}_i$ of the ith sphere to the forces,

$$\dot{\mathbf{x}}_1 = M_{11}\cdot\mathbf{f}_1 + M_{12}\cdot\mathbf{f}_2 + M_{13}\cdot\mathbf{f}_3,$$

$$\dot{\mathbf{x}}_2 = M_{21}\cdot\mathbf{f}_1 + M_{22}\cdot\mathbf{f}_2 + M_{23}\cdot\mathbf{f}_3,$$

$$\dot{\mathbf{x}}_3 = M_{31}\cdot\mathbf{f}_1 + M_{32}\cdot\mathbf{f}_2 + M_{33}\cdot\mathbf{f}_3. \tag{6}$$

In the above set of equations, the key role of mobility tensor (2) and self-mobility tensor (5) is quite manifest. As long as no external force or external torque is applied to the system, the swimmer is force and torque free. Thus,

$$\mathbf{f}_1 + \mathbf{f}_2 + \mathbf{f}_3 = 0,$$

$$\boldsymbol{\tau}_1 + \boldsymbol{\tau}_2 + \boldsymbol{\tau}_3 = 0, \tag{7}$$

where $\boldsymbol{\tau}_1 = 0$, $\boldsymbol{\tau}_2 = (\mathbf{x}_2 - \mathbf{x}_1)\times\mathbf{f}_2$, $\boldsymbol{\tau}_3 = (\mathbf{x}_3 - \mathbf{x}_1)\times\mathbf{f}_3$, and $\times$ denotes the outer product.

To make a complete system of equations, geometrical constrains describing the internal motion of the swimmer should be considered. Time-dependent functions $g(t)$ and $h(t)$ show the arm length dynamics. Thus,

$$\mathbf{x}_1 - \mathbf{x}_3 = h(t)\hat{t},$$

$$\mathbf{x}_2 - \mathbf{x}_1 = g(t)\hat{t}, \tag{8}$$

where the arm direction is denoted by the unit vector $\hat{t} = \cos\theta\hat{x} + \sin\theta\hat{z}$. θ denotes the direction of swimming (see Fig. 1).

In the following, we study the swimmer motion when the arm lengths change around a mean value L, i.e.,

$$g(t) = L + u_1(t),$$

$$h(t) = L + u_2(t). \tag{9}$$

The average of periodic functions $u_1(t)$ and $u_2(t)$ is zero. We will express the overall dynamics of swimmer in terms of the internal motions given by $u_1(t)$ and $u_2(t)$. The average translational velocity $\mathbf{v}$ and angular velocity $\dot{\theta} = d\theta/dt$ of swimmer are of particular interest,

$$\mathbf{v} = M_{11}\cdot\mathbf{f}_1 + M_{12}\cdot\mathbf{f}_2 + M_{13}\cdot\mathbf{f}_3,$$

$$\dot{\theta} = \frac{1}{h}\hat{n}\cdot[(M_{11} - M_{31})\cdot\mathbf{f}_1 + (M_{12} - M_{32})\cdot\mathbf{f}_2 + (M_{13} - M_{33})\cdot\mathbf{f}_3], \tag{10}$$

where $\hat{n} = -\sin\theta\hat{x} + \cos(\theta)\hat{z}$ is a unit vector perpendicular to the arms.

Governing Eqs. (6)–(8) can be written in the following form:

$$a_{11}f_{2x} + a_{12}f_{2z} + a_{13}f_{3x} + a_{14}f_{3z} = \dot{g},$$

$$a_{21}f_{2x} + a_{22}f_{2z} + a_{23}f_{3x} + a_{24}f_{3z} = \dot{h},$$

$$a_{31}f_{2x} + a_{32}f_{2z} + a_{33}f_{3x} + a_{34}f_{3z} = 0,$$

$$a_{41}f_{2x} + a_{42}f_{2z} + a_{43}f_{3x} + a_{44}f_{3z} = 0. \tag{11}$$

Matrix elements a_{ij} are given in the Appendix. Note that $\mathbf{f}_1 = -\mathbf{f}_2 - \mathbf{f}_3$, $\mathbf{v}$, and $\dot{\theta}$ are already expressed in terms of the above force components. Matrix elements a_{ij} have a strong nonlinear dependence on coordinates x_i, z_i, and angle θ. However, in two limiting cases, we can provide *analytical* expressions for the force and velocity vectors.

A. Swimming far from the wall

In the limit $z\to\infty$, we are dealing with a swimmer in free space [16]. To study swimming far from the wall, i.e., quite farther than the largest length of swimmer, it is advisable to introduce the small dimensionless parameter $\varepsilon = L/z$ and expand forces, velocities, and so on, in powers of ε,

$$\mathbf{f}_i = \mathbf{f}_i^{(0)} + \mathbf{f}_i^{(1)} + \mathbf{f}_i^{(2)} + \mathcal{O}(\varepsilon^3). \tag{12}$$

We also expand matrix $A = [a_{ij}]$ in powers of ε and solve Eq. (11) using the standard perturbation methods.

We duplicate the results known for a free swimmer at the zeroth order of ε. Following [16,20], we do further simplifications by assuming that all the arm length variations u_1 and u_2 and sphere size a are much smaller than the average arm length L. Thus, we only keep leading terms. Averaging the final results over a complete period of deformations, we find that

$$\mathbf{f}_1^{(0)} = \frac{5}{4}\pi\eta\left(\frac{a}{L}\right)^2\Phi\hat{t},$$

$$\mathbf{f}_2^{(0)} = -\frac{5}{8}\pi\eta\left(\frac{a}{L}\right)^2\Phi\hat{t},$$

$$\mathbf{f}_3^{(0)} = -\frac{5}{8}\pi\eta\left(\frac{a}{L}\right)^2\Phi\hat{t}, \tag{13}$$

where

$$\Phi = \langle(u_1\dot{u}_2 - u_2\dot{u}_1)\rangle. \tag{14}$$

Here $\langle\ \rangle$ denotes averaging over a complete period of deformations. Φ is proportional to the area enclosed by the path corresponding to the nonreciprocal internal motion (see Fig.

1). For a simple elliptic path in the deformation space, $u_1(t)=u_{10}\cos(\omega t)$, $u_2(t)=u_{20}\cos(\omega t+\phi)$, and $\Phi=-\omega u_{10}u_{20}\sin(\phi)$.

Equation (13) shows that the hydrodynamic forces exerted on free swimmer are along the arm direction $\hat{t}$. The force distribution on the spheres represents a force quadrupole. This observation means that the far-field distribution of fluid velocity resembles the velocity field of a single force quadrupole. This is believed to be a universal nature of symmetric low-Reynolds-number swimmers [19].

We also find that

$$\mathbf{v}^{(0)}=-\frac{7}{24}\frac{a}{L^2}\Phi\hat{t},$$

$$\dot{\theta}^{(0)}=0. \tag{15}$$

The free swimmer moves in the direction determined by both the initial angle θ and phase difference ϕ between arm deformations. Note that two swimmers, one with parameters θ and Φ and another with the same labels for its spheres but with parameters $\theta+\pi$ and $-\Phi$ are equivalent. Equations (15) demonstrate this equivalence.

The influence of wall on a far swimmer is represented in the higher-order terms of the expansion (12). Quite remarkably, all corrections of the first order in $\varepsilon=L/z$, i.e., $\mathbf{f}_i^{(1)}$, $\mathbf{v}^{(1)}$, and $\dot{\theta}^{(1)}$ are zero. The second-order correction of hydrodynamic forces are given by

$$\mathbf{f}_1^{(2)}=\frac{3}{16}\pi\eta\left(\frac{a}{L}\right)^2\left(\frac{L}{z}\right)^2\Phi\cos\theta\hat{n},$$

$$\mathbf{f}_2^{(2)}=-\frac{3}{32}\pi\eta\left(\frac{a}{L}\right)^2\left(\frac{L}{z}\right)^2\Phi\cos\theta\hat{n},$$

$$\mathbf{f}_3^{(2)}=-\frac{3}{32}\pi\eta\left(\frac{a}{L}\right)^2\left(\frac{L}{z}\right)^2\Phi\cos\theta\hat{n}. \tag{16}$$

Thus, the effect of a distant wall appears as a quadrupole force distribution with an *angle-dependent strength*. A swimmer moving parallel to the wall experiences a large force quadrupole, while one moving perpendicular to the wall experiences no force quadrupole. Remarkably, the wall-induced forces are *perpendicular* to the arms of swimmer. Note that a free swimmer experiences hydrodynamic forces parallel to its arms.

Now we focus on swimmer's translational and angular velocities. After expanding our results for small radius limit and averaging over a complete period of internal motion, we find

$$\mathbf{v}^{(2)}=\frac{1}{8}\frac{a}{L^2}\left(\frac{L}{z}\right)^2\Phi\cos\theta\hat{n},$$

$$\dot{\theta}^{(3)}=\frac{1}{128}\frac{a}{L^3}\left(\frac{L}{z}\right)^3\Phi[18\sin(2\theta)+\sin(4\theta)]. \tag{17}$$

We define the intrinsic direction of swimmer as the direction of motion in the absence of wall. The intrinsic direction is $\hat{t}$ when $\Phi<0$. In this case, $\theta<0$ ($\theta>0$) means that the swimmer is moving toward (away from) the $z=0$ plane. In the presence of wall, $\dot{\theta}^{(1)}=\dot{\theta}^{(2)}=0$, but $\dot{\theta}^{(3)}\neq 0$. However, Eq. (17) reveals that $\theta=0$ is a *stable* configuration. In other words, the swimmer prefers to reorient itself and move parallel to the wall. Equation (17) also shows that the wall-induced translational velocity of swimmer is angle dependent and perpendicular to the arms. Note that the velocity of free swimmer is angle independent and parallel to the arms. We also note that Eq. (17) demonstrates the equivalence between two swimmers: one with parameters θ and Φ and other with parameters $\theta+\pi$ and $-\Phi$.

B. Swimming close to the wall

In view of designing a robust drug carrier moving in capillaries, we pay attention to the three-sphere swimmer near a wall. In this limit, the distance z to the wall is less than the arm length L (see Fig. 1). However, we assume that $z>L\sin\theta$, i.e., the swimmer does not touch the wall. In order to have clear and illuminating results, it is quite appropriate to expand expressions in powers of z/L and keep only leading terms. Notably, the mobility matrix assumes a simple form,

$$M_{ij}=\frac{3}{2\pi\eta}\frac{z_iz_j}{(x_i-x_j)^3}\begin{pmatrix}1&0\\0&0\end{pmatrix}. \tag{18}$$

As before, we rely on the plausible assumption that $u_1(t)$, $u_2(t)$, and a are much smaller than L. Expanding expressions in powers of a, we deliberately treat μ_0 as a constant since the term proportional to a/z exhibits the distance dependence of self-mobility tensor (5).

For small values of θ, i.e., when the swimmer is almost parallel to the wall, we find

$$f_{1x}=\frac{9}{8}\pi\eta\left(\frac{a}{L}\right)^2\left[-\frac{2}{6}\theta^2+17\left(\frac{z}{L}\right)^2\right]\Phi,$$

$$f_{1z}=0,$$

$$f_{2x}=\frac{9}{8}\pi\eta\left(\frac{a}{L}\right)^2\left[\frac{1}{6}\theta^2+19\theta\frac{z}{L}-\frac{17}{2}\left(\frac{z}{L}\right)^2\right]\Phi,$$

$$f_{2z}=0,$$

$$f_{3x}=\frac{9}{8}\pi\eta\left(\frac{a}{L}\right)^2\left[\frac{1}{6}\theta^2-19\theta\frac{z}{L}-\frac{17}{2}\left(\frac{z}{L}\right)^2\right]\Phi,$$

$$f_{3z}=0. \tag{19}$$

Since $\hat{t}\approx\hat{x}$ and $\hat{n}\approx\hat{z}$ for small values of θ, we observe that the wall-induced forces are parallel to the arms of swimmer. Moreover, $f_{2x}\neq f_{3x}$, i.e., the force distribution on the spheres represents a force *dipole*. Note that in the far regime, the force distribution represents a force quadrupole.

We also find

$$v_x = -\frac{1}{16}\left(\frac{a}{L^2}\right)\left[\theta^2 + 93\left(\frac{z}{L}\right)^2\right]\Phi,$$

$$v_z = \frac{3}{16}\left(\frac{a}{L^2}\right)\left[\theta^3 - \theta\left(\frac{z}{L}\right)^2\right]\Phi,$$

$$\dot{\theta} = \frac{105}{16}\left(\frac{a}{L^3}\right)\theta^2\left(\frac{z}{L}\right)\Phi. \quad (20)$$

The swimmer velocity vector has a big (small) component parallel (perpendicular) to its arm. Note that when the swimmer is far from (close to) the wall, the velocity is proportional to $1/L^2$ $(1/L^4)$. The increase in arm length in fact reduces the swimmer's speed near the wall. Equations (15) and (20) also show that $v_{\text{close}} = 19.93(z/L)^2 v_{\text{free}}$ when $\theta = 0$, i.e., the velocity decreases quadratically on approaching the wall.

Now assume that $\Phi < 0$ and $\hat{t}$ represents the intrinsic direction of swimmer. The above dynamical equations show that the angle θ decreases in the presence of wall. Moreover, on decreasing the angle θ below zero, the distance z between swimmer and wall increases. In other words, a swimmer whose arms make a slight positive (negative) angle with the horizon tends (does not tend) to make itself parallel to the plate. This clearly shows that a swimmer near to the wall is sensitive to external noise and perturbations.

Note that to have a better picture of the swimmer's instability and to investigate its collision with the wall, the self-mobility tensors (5) should be refined when z and a are comparable [30].

V. DISCUSSION AND CONCLUDING REMARKS

In this paper, we investigate the influence of a rigid wall on the dynamics of a low-Reynolds-number three-sphere swimmer. We present analytical results for hydrodynamic forces, translational, and angular velocities of a swimmer distant from or close to the wall.

A far swimmer whose arm makes an angle θ with the horizon experiences the wall presence as an angle-dependent quadrupole force proportional to $(a/L)^2(L/z)^2\cos\theta$. The wall-induced forces and translational velocity are perpendicular to the arms of swimmer. A far swimmer prefers to orient its arms parallel to the plate. This state is stable. Quite remarkably, the parallel state is unstable when the swimmer is close to the wall. The swimmer orients its head toward the wall when the initial angle θ is slightly negative. For small values of θ, the wall-induced forces are parallel to the arms and make a force dipole.

For a swimmer at an arbitrary distance from the wall, we perform a numerical analysis of the governing Eq. (11), keeping the whole terms of matrix elements M_{ij} and a_{ij} quoted in the Appendix. The obtained numerical results confirm our analytical findings for swimming far from or close to the wall. Moreover, the numerical analysis reveals that for which initial values of scaled distance z/L and angle $\theta < 0$, the swimmer is in the far phase F or near phase N. For $z > 3L$, it is plausible to assume that the swimmer is far from the wall (see Fig. 2). For most initial conditions $\theta > 0$, a swimmer far from or close to the wall orients itself parallel to the wall. This positive angle phase P is delineated in Fig. 2. Our numerical analysis also shows the existence of an intermediate phase I. The swimmer has a complicated and even chaotic behavior. Depending on the initial angle θ, the distance z between swimmer and wall either increases or decreases (see Fig. 3). Note that in the phase N, the distance z always increases. Long dashed lines in Fig. 2 show the region $z < L \sin\theta$ where the swimmer touches the wall.

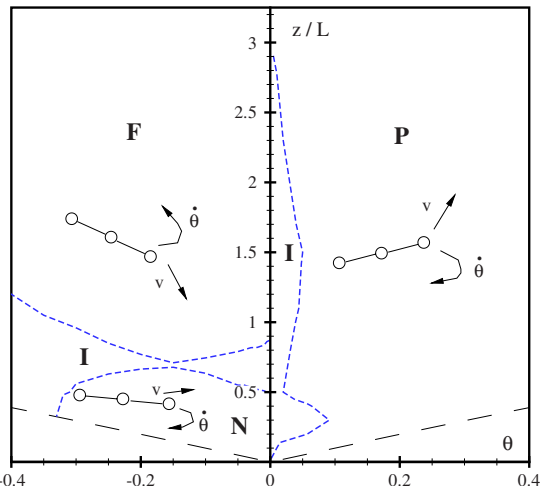

FIG. 2. (Color online) Phase diagram for a low-Reynolds-number three-sphere swimmer moving adjacent to a wall. Phase F: a far swimmer prefers to orient its arms parallel to the plate. Phase N: when a swimmer is close to the wall, θ decreases but z increases. Phase P: a swimmer far from or close to the wall orients itself parallel to the wall. Phase I: depending on the initial angle θ, the distance z between swimmer and wall either increases or decreases. Long dashed lines show the region $z < L \sin\theta$, where the swimmer touches the wall.

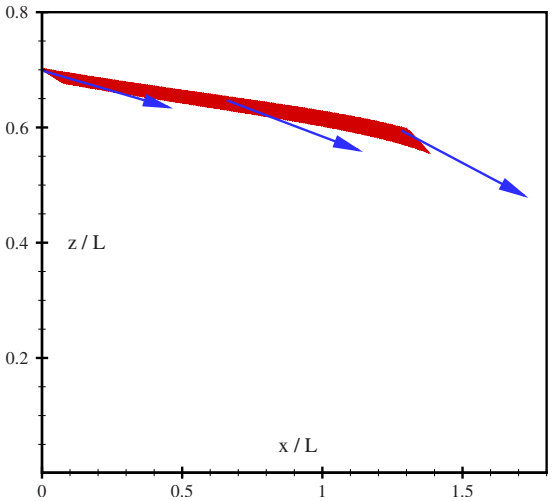

FIG. 3. (Color online) Trajectory of a swimmer when $a/L = 0.01$, $u_{10}/L = u_{20}/L = 0.1$, $\phi = \pi/2$, and initial conditions are $z(0)/L = 0.7$ and $\theta(0) = -0.3$ in radian. Note that the distance z between swimmer and wall decreases as θ decreases. On approaching the wall, the swimmer's fluctuation along the vertical axis increases.

Our work can be extended in many directions. Our results can be examined by a simple extension of the recent experiment of Leoni *et al.* [23]. Swimming in a complex geometry, e.g., a microchannel of rectangular or circular cross section is of immediate interest. Inspired by the colonies of swimming bacteria near biological membranes, we are investigating many propellers adjacent to a wall.

APPENDIX: HYDRODYNAMIC MOBILITY TENSORS

The hydrodynamic mobility tensors appearing in Eq. (6) are

$$M_{ij}^{xx}=\frac{1}{8\pi\eta}\left[\frac{1}{r}-\frac{1}{R}+(x_i-x_j)^2\left(\frac{1}{r^3}-\frac{1}{R^3}\right)+2z_j^2\left(\frac{1}{R^3}-\frac{3(x_i-x_j)^2}{R^5}\right)-2z_j\left(\frac{(z_i+z_j)}{R^3}-\frac{3(x_i-x_j)^2(z_i+z_j)}{R^5}\right)\right],$$

$$M_{ij}^{xz}=\frac{1}{8\pi\eta}\left[\frac{(x_i-x_j)(z_i-z_j)}{r^3}-\frac{(x_i-x_j)(z_i+z_j)}{R^3}+6z_j^2\frac{(x_i-x_j)(z_i+z_j)}{R^5}+2z_j\left(\frac{(x_i-x_j)}{R^3}-\frac{3(x_i-x_j)(z_i+z_j)^2}{R^5}\right)\right],$$

$$M_{ij}^{zx}=\frac{1}{8\pi\eta}\left[\frac{(x_i-x_j)(z_i-z_j)}{r^3}-\frac{(x_i-x_j)(z_i+z_j)}{R^3}-6z_j^2\frac{(x_i-x_j)(z_i+z_j)}{R^5}+2z_j\left(\frac{(x_i-x_j)}{R^3}+\frac{3(x_i-x_j)(z_i+z_j)^2}{R^5}\right)\right],$$

$$M_{ij}^{zz}=\frac{1}{8\pi\eta}\left[\frac{1}{r}-\frac{1}{R}+\frac{(z_i-z_j)^2}{r^3}-\frac{(z_i+z_j)^2}{R^3}-2z_j^2\left(\frac{1}{R^3}-\frac{3(z_i+z_j)^2}{R^5}\right)+2z_j\left(\frac{(z_i+z_j)}{R^3}-\frac{3(z_i+z_j)^3}{R^5}\right)\right],$$

where $r^2=(x_i-x_j)^2+(z_i-z_j)^2$ and $R^2=(x_i-x_j)^2+(z_i+z_j)^2$.

We define

$$S_1=M_{12}+M_{21}-M_{11}-M_{22},$$

$$S_2=M_{13}+M_{21}-M_{11}-M_{23},$$

$$S_3=M_{12}+M_{31}-M_{11}-M_{32},$$

$$S_4=M_{13}+M_{31}-M_{11}-M_{33}.$$

Now the matrix elements appearing in Eq. (11) can be introduced as

$$a_{11}=-\cos\theta S_1^{xx}-\sin\theta S_1^{zx},$$

$$a_{12}=-\cos\theta S_1^{xz}-\sin\theta S_1^{zz},$$

$$a_{13}=-\cos\theta S_2^{xx}-\sin\theta S_2^{zx},$$

$$a_{14}=-\cos\theta S_2^{xz}-\sin\theta S_2^{zz},$$

$$a_{21}=\cos\theta S_3^{xx}+\sin\theta S_3^{zx},$$

$$a_{22}=\cos\theta S_3^{xz}+\sin\theta S_3^{zz},$$

$$a_{23}=\cos\theta S_4^{xx}+\sin\theta S_4^{zx},$$

$$a_{24}=\cos\theta S_4^{xz}+\sin\theta S_4^{zz},$$

$$a_{31}=\cos\theta(hS_1^{zx}+gS_3^{zx})-\sin\theta(hS_1^{xx}+gS_3^{xx}),$$

$$a_{32}=\cos\theta(hS_1^{zz}+gS_3^{zz})-\sin\theta(hS_1^{xz}+gS_3^{xz}),$$

$$a_{33}=\cos\theta(hS_2^{zx}+gS_4^{zx})-\sin\theta(hS_2^{xx}+gS_4^{xx}),$$

$$a_{34}=\cos\theta(hS_2^{zz}+gS_4^{zz})-\sin\theta(hS_2^{xz}+gS_4^{xz}),$$

$$a_{41}=g\sin\theta,$$

$$a_{42}=-g\cos\theta,$$

$$a_{43}=-h\sin\theta,$$

$$a_{44}=h\cos\theta.$$

[1] E. R. Kay, D. A. Leigh, and F. Zerbetto, Angew. Chem., Int. Ed. **46**, 72 (2007); K. Kinbara and T. Aida, Chem. Rev. (Washington, D.C.) **105**, 1377 (2005).

[2] J. P. Sauvage and V. Amendola, *Molecular Machines and Motors* (Springer-Verlag, Berlin, 2001).

[3] V. Balzani *et al.*, Angew. Chem., Int. Ed. **39**, 3348 (2000).

[4] S. H. Kim, J. H. Jeong, S. H. Lee, S. W. Kim, and T. G. Park, J. Controlled Release **129**, 107 (2008).

[5] P. S. Dittrich and A. Manz, Nat. Rev. Drug Discovery **5**, 210 (2006).

[6] H. Bruus, *Theoretical Microfluidics* (Oxford University Press, Oxford, 2008).

[7] H. C. Berg, *E. coli in Motion* (Springer, New York, 2004).

[8] G. Taylor, Proc. R. Soc. London, Ser. A **209**, 447 (1951).

[9] E. M. Purcell, Am. J. Phys. **45**, 3 (1977).

[10] L. E. Becker, S. A. Koehler, and H. A. Stone, J. Fluid Mech. **490**, 15 (2003).

[11] D. Tam and A. E. Hosoi, Phys. Rev. Lett. **98**, 068105 (2007).

[12] J. E. Avron, O. Gat, and O. Kenneth, Phys. Rev. Lett. **93**, 186001 (2004); J. E. Avron, O. Kenneth, and D. H. Oaknin,

New J. Phys. **7**, 234 (2005).
[13] B. U. Felderhof, Phys. Fluids **18**, 063101 (2006).
[14] W. F. Paxton *et al.*, Angew. Chem., Int. Ed. **45**, 5420 (2006); J. Am. Chem. Soc. **126**, 13424 (2004); S. Fournier-Bidoz *et al.*, Chem. Commun. (Cambridge) 2005, 441 (2005); N. Mano and A. Heller, J. Am. Chem. Soc. **127**, 11574 (2005); R. Golestanian, T. B. Liverpool, and A. Ajdari, Phys. Rev. Lett. **94**, 220801 (2005); J. R. Howse, R. A. L. Jones, A. J. Ryan, T. Gough, R. Vafabakhsh, and R. Golestanian, *ibid.* **99**, 048102 (2007); G. Rückner and R. Kapral, *ibid.* **98**, 150603 (2007).
[15] R. Dreyfus, J. Baudry, M. L. Roper, M. Fermigier, H. A. Stone, and J. Bibette, Nature (London) **437**, 862 (2005); E. Gauger and H. Stark, Phys. Rev. E **74**, 021907 (2006); E. M. Gauger, M. T. Downton, and H. Stark, Eur. Phys. J. E **28**, 231 (2009).
[16] A. Najafi and R. Golestanian, Phys. Rev. E **69**, 062901 (2004).
[17] Note that a swimmer with *two* rigid spheres connected by one arm has *one* internal degree of freedom and cannot make net translational progress. As pointed out in Ref. [12], the net translational motion is possible if two spheres change their volumes as well as their distance.
[18] D. J. Earl *et al.*, J. Chem. Phys. **126**, 064703 (2007).
[19] C. M. Pooley, G. P. Alexander, and J. M. Yeomans, Phys. Rev. Lett. **99**, 228103 (2007); G. P. Alexander, C. M. Pooley, and J. M. Yeomans, Phys. Rev. E **78**, 045302(R) (2008).
[20] R. Golestanian and A. Ajdari, Phys. Rev. E **77**, 036308 (2008).
[21] R. Golestanian and A. Ajdari, Phys. Rev. Lett. **100**, 038101 (2008).
[22] R. Golestanian, Eur. Phys. J. E **25**, 1 (2008).
[23] M. Leoni, J. Kotar, B. Bassetti, P. Cicuta, and M. C. Lagomarsino, Soft Matter **5**, 472 (2009).
[24] H. H. Wensink and H. Löwen, Phys. Rev. E **78**, 031409 (2008); S. van Teeffelen and H. Löwen, *ibid.* **78**, 020101(R) (2008).
[25] C. Sendner and R. R. Netz, EPL **79**, 58004 (2007).
[26] J. P. Hernandez-Ortiz, C. G. Stoltz, and M. D. Graham, Phys. Rev. Lett. **95**, 204501 (2005).
[27] P. Tierno, R. Golestanian, I. Pagonabarraga, and F. Sagues, Phys. Rev. Lett. **101**, 218304 (2008).
[28] R. M. Harshey, Annu. Rev. Microbiol. **57**, 249 (2003).
[29] P. D. Frymier, R. M. Ford, H. C. Berg, and P. T. Cummings, Proc. Natl. Acad. Sci. U.S.A. **92**, 6195 (1995).
[30] J. Happel and H. Brenner, *Low Reynolds Number Hydrodynamics* (Noordhoff, Leyden, 1973).
[31] A. Pralle *et al.*, Appl. Phys. A: Mater. Sci. Process. **66**, S71 (1998).
[32] A. P. Berke, L. Turner, H. C. Berg, and E. Lauga, Phys. Rev. Lett. **101**, 038102 (2008).
[33] L. Rothschild, Nature (London) **198**, 1221 (1963).
[34] H. Winet, G. S. Bernstein, and J. Head, J. Reprod. Fertil. **70**, 511 (1984).
[35] G. Harkes, J. Dankert, and J. Feijen, Appl. Environ. Microbiol. **58**, 1500 (1992).
[36] J. T. Gannon, V. B. Manilal, and M. Alexander, Appl. Environ. Microbiol. **57**, 190 (1991); R. E. Martin, E. J. Bouwer, and L. M. Hanna, Environ. Sci. Technol. **26**, 1053 (1992).
[37] H. C. Berg and L. Turner, Biophys. J. **58**, 919 (1990).
[38] J. R. Blake, Proc. Cambridge Philos. Soc. **70**, 303 (1971).
[39] Y. W. Kim and R. R. Netz, J. Chem. Phys. **124**, 114709 (2006).